ACS Photonics

Article

Cite This: ACS Photonics 2018, 5, 3305−3314

Graded-Index Separate Confinement Heterostructure AlGaN Nanowires: Toward Ultraviolet Laser Diodes Implementation

Haiding Sun,*,† Davide Priante,‡ Jung-Wook Min,‡ Ram Chandra Subedi,‡ Mohammad Khaled Shakfa,‡ Zhongjie Ren,† Kuang-Hui Li,† Ronghui Lin,† Chao Zhao,‡ Tien Khee Ng,‡ Jae-Hyun Ryou,§ Xixiang Zhang,∥ Boon S. Ooi,*,‡ and Xiaohang Li*,†

King Abdullah University of Science and Technology (KAUST), †Computer, Electrical, and Mathematical Sciences and Engineering Division, Advanced Semiconductor Laboratory, ‡Computer, Electrical, and Mathematical Sciences and Engineering Division, Photonics Laboratory, and ∥Division of Physical Science and Engineering, Thuwal 23955-6900, Saudi Arabia

§Department of Mechanical Engineering, Material Science and Engineering Program, Texas Center for Superconductivity at UH (TcSUH), and Advanced Manufacturing Institute (AMI), University of Houston, Houston, Texas 77204-4006, United States

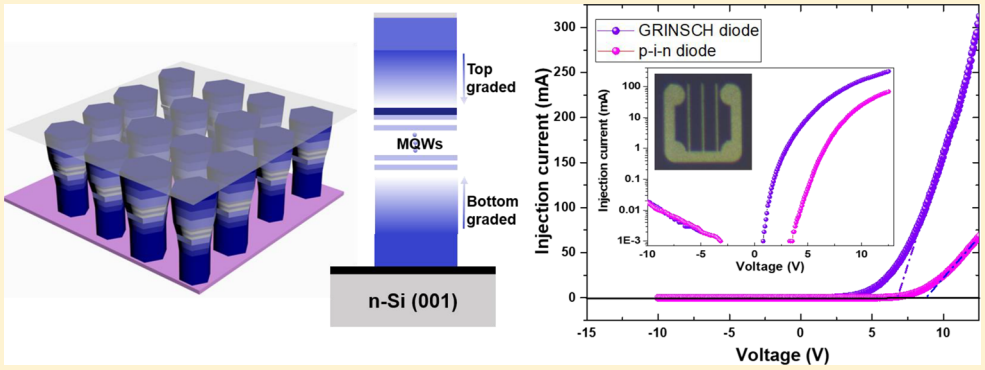

ABSTRACT: High-density dislocations in materials and poor electrical conductivity of p-type AlGaN layers constrain the performance of the ultraviolet light emitting diodes and lasers at shorter wavelengths. To address those technical challenges, we design, grow, and fabricate a novel nanowire structure adopting a graded-index separate confinement heterostructure (GRINSCH) in which the active region is sandwiched between two compositionally graded AlGaN layers, namely, a GRINSCH diode. Calculated electronic band diagram and carrier concentrations show an automatic formation of a p−n junction with electron and hole concentrations of ∼10^{18} /cm^3 in the graded AlGaN layers without intentional doping. The transmission electron microscopy experiment confirms the composition variation in the axial direction of the graded AlGaN nanowires. Significantly lower turn-on voltage of 6.5 V (reduced by 2.5 V) and smaller series resistance of 16.7 Ω (reduced by nearly four times) are achieved in the GRINSCH diode, compared with the conventional p-i-n diode. Such an improvement in the electrical performance is mainly attributed to the effectiveness of polarization-induced n- and p-doping in the compositionally graded AlGaN layers. In consequence, the carrier transport and injection efficiency of the GRINSCH diode are greatly enhanced, which leads to a lower turn-on voltage, smaller series resistance, higher output power, and enhanced device efficiency. The calculated carrier distributions (both electrons and holes) across the active region show better carrier confinement in the GRINSCH diode. Thus, together with the large optical confinement, the GRINSCH diode could offer an unconventional path for the development of solid-state ultraviolet optoelectronic devices, mainly laser diodes of the future.

KEYWORDS: *aluminum gallium nitride nanowire, graded index, polarization doping, ultraviolet laser*

The ultraviolet light emitting devices, for example, light emitting diodes (LEDs) and lasers, are critical in a variety of applications, including medical diagnostics, UV curing, optical non-line-of-sight communications, and water/air sterilization.[1] Those devices, made of aluminum gallium nitride (AlGaN) semiconductors that possess large and tunable bandgap from 3.4 to 6.1 eV and are chemically robust, have a long lifetime, and are operationally stable, making them one of the top contenders to replace the current UV gas lasers and toxic, power consuming, and eco-unfriendly mercury-based UV lamps.[1,2] As the operation wavelength requirements of the UV sources move toward shorter wavelengths, Al-rich AlGaN layers are indispensable in design and fabrication of the devices. However, Al-rich AlGaN layers suffer from a series of challenges in realizing highly crystalline material with efficient doping, which so far results in poor device performance characteristics.[3] Deteriorated crystalline quality, resulting from the lattice-mismatched foreign substrate and short diffusion length of Al adatoms on a growing surface, is often observed

Received: April 25, 2018
Published: June 19, 2018

DOI: 10.1021/acsphotonics.8b00538
ACS Photonics 2018, 5, 3305−3314

during the deposition of Al-rich AlGaN epitaxial layers. The generated crystalline defects (dislocations) result in high leakage currents and suppress the radiative recombination efficiency in the active region, which severely impact the device operation.[4,5] Furthermore, high-conductivity p-type Al-rich AlGaN layers by Mg doping are difficult to obtain because of the low doping efficiency due to the high activation energy of the acceptor.[6,7] Therefore, the threshold operating voltage and device series resistance of reported UV laser diodes are quite high. For instance, Yoshida et al. have demonstrated UV lasers at 336 and 342 nm, which are the shortest wavelengths of laser diodes with high output power (>1 mW) to date.[8,9] However, the operating voltages for both laser diodes surpass 25 V in the lasing mode due to poor hole injection efficiency.

Many approaches have been attempted to improve the conductivity of the layers by utilizing Mg doping in $Al_xGa_{1-x}N/Al_yGa_{1-y}$ N superlattices,[10−13] Mg delta doping,[14−16] and tunnel-junction injection of nonequilibrium holes.[17,18] In particular, a high sheet carrier density at the interface of the $Al_xGa_{1-x}N/Al_yGa_{1-y}$ N heterojunction was theoretically predicted and experimentally demonstrated.[19] Two-dimensional (2D) electron or hole gas can be generated for high power transistor applications.[19−21] Most importantly, polarization-induced three-dimensional (3D) electron and hole gases can be created by introducing a compositional AlGaN grading profile, instead of an abrupt AlGaN heterojunction.[22−25] Such 3D free electrons and holes usually originate from donor- and acceptor-like impurities or defects via polarization-induced ionization process and have been implemented in AlGaN-based planar UV emitters[26−28] without any intentional doping.[23]

Compared to the AlGaN epitaxial thin-film layers, p-type AlGaN nanowires were recently found to have lower resistivity owing to more efficient Mg incorporation and lower activation energy which are caused by the reduced lattice strain imposed by surface dopants, compared to bulk dopants.[29−31] This observation is consistent with earlier discoveries that semiconductor nanowires often have higher doping efficiency than thin-film layers, such as InN,[32] Si, and Ge nanowires.[33−37] Furthermore, due to the efficient strain relaxation associated with the large surface-to-volume ratio, nearly defect-free AlGaN nanowires can be grown directly on many substrates.[38,39] Hence, the development of new UV sources made of AlGaN nanowires have been a field of high interest. In this context, polarization-induced doping together with the distinctly better electrical conductivity of p-type Al-rich AlGaN nanowires has been suggested to address the material challenges, for example, high-density dislocations and low p-doping efficiency in the AlGaN layers. However, only a few attempts have been made.[40,41] In these efforts, nanowire structures were grown by molecular beam epitaxy (MBE) under N-rich conditions, and the polarization-induced doping was realized by linearly grading the structure from GaN to AlN and then from AlN to GaN. However, such direct grading from GaN to AlN nanowires leads to polarization-induced hole doping due to the nature of N-polarity of the nanowires, forcing those nanowires to start with p-type on a p-type substrate (e.g., p-Si). The nanowire-based devices with such a "bottom p-type" structure raises several issues: (1) p-Si has a substantial valence band offset with p-GaN, resulting in poor hole injection into the active region of the device; (2) a memory effect of Mg dopant could deteriorate the performance of devices grown by both MBE and metalorganic chemical vapor deposition (MOCVD); (3) p-type substrates have poor electrical performance than n-type. Furthermore, an amorphous insulating SiN_x layer is often observed when nanowires were grown directly on Si,[42,43] increasing the interfacial resistance, thus, requiring a higher device operating voltage.

Here, we design, grow, and characterize AlGaN nanowires on metal-coated n-Si substrates in the form of graded-index separate confinement heterostructure (GRINSCH). A Ti/TaN metal-bilayer is deposited on n-Si prior to the nanowire growth to avoid the formation of the insulating SiN_x layer.[44] The compositional gradient of Al content along the growth direction is carefully designed and controlled. For comparison, nanowires with a conventional p-i-n diode configuration are also prepared. Detailed optical and electrical studies of both structures are carried out. We demonstrate the superior performance of GRINSCH diodes compared to the conventional p-i-n counterparts. In the end, it is recognized that the GRINSCH diodes could offer a unique structure for the realization of efficient UV emitters and, most importantly, their potentials in the implementation of UV laser diode owing to a better carrier and optical confinement.

EXPERIMENTAL SECTION

The nanowires studied in this work were grown by a Veeco GEN-930 plasma-assisted molecular beam epitaxy. Prior to the AlGaN nanowire growth, a ∼20 nm TaN diffusion barrier was deposited on a (100) n-type Si substrate (10^{-1} Ω·cm) using atomic layer deposition (ALD) at 300 °C. A precursor was purged with Ar (200 sccm) and H_2 plasma (50 sccm) during the deposition, followed by a ∼100 nm Ti layer deposited by an e-beam evaporator. Our previous study shows that by inserting a 20 nm TaN interlayer between a Ti preorienting layer and the Si substrate, we were able to improve carrier injection and nanowire uniformity.[44] Furthermore, this Ti/TaN metal-bilayer can also inhibit the Ti/Si interdiffusion, which can cause surface delamination during the nanowire nucleation at high growth temperatures. Such surface delamination leads to an extremely rough surface and causes a nonuniform growth of the nanowires (the height of nanowires varies in a range of ∼100 nm).[45,46] By inserting the TaN interlayer, the surface roughness of Ti/TaN metal-bilayer-coated Si can be as low as 1.6 nm, and thus, the nanowires grown on top have high density and aligned well vertically with similar height, making the additional surface planarization process unnecessary.[44] After metal coating, the Ti/TaN/Si substrate was then outgassed in the MBE load lock at 200 °C for 1 h (h) followed by outgassing in the buffer chamber at 600 °C for 2 h to remove moisture and molecular adsorption for subsequent growth. For the nanowire growth, first of all, Si-doped n-GaN seeds were initiated at a substrate temperature of 485 °C for 1 min to reduce Ga adatom desorption and increase the nucleation probability. The Ga beam equivalent pressure (BEP) was 6.0×10^{-8} Torr, the Si effusion cell was kept at 1180 °C, and the high-brightness nitrogen plasma was sustained using 350 W RF power and 1-sccm flow rate. In this condition, less than 3 nm of n-GaN was grown. The temperature was then raised to 630 °C to grow a bottom n-AlGaN layer. We estimated the nominal Al composition based on the ratio of the Al BEP to Ga BEP. The active region is composed of 10 stacked repetitions of alternating $Al_xGa_{1-x}N$ quantum well(QW) with Al and Ga BEPs of 2.0×10^{-8} and 5.5×10^{-8} Torr, respectively,

DOI: 10.1021/acsphotonics.8b00538
ACS Photonics 2018, 5, 3305−3314

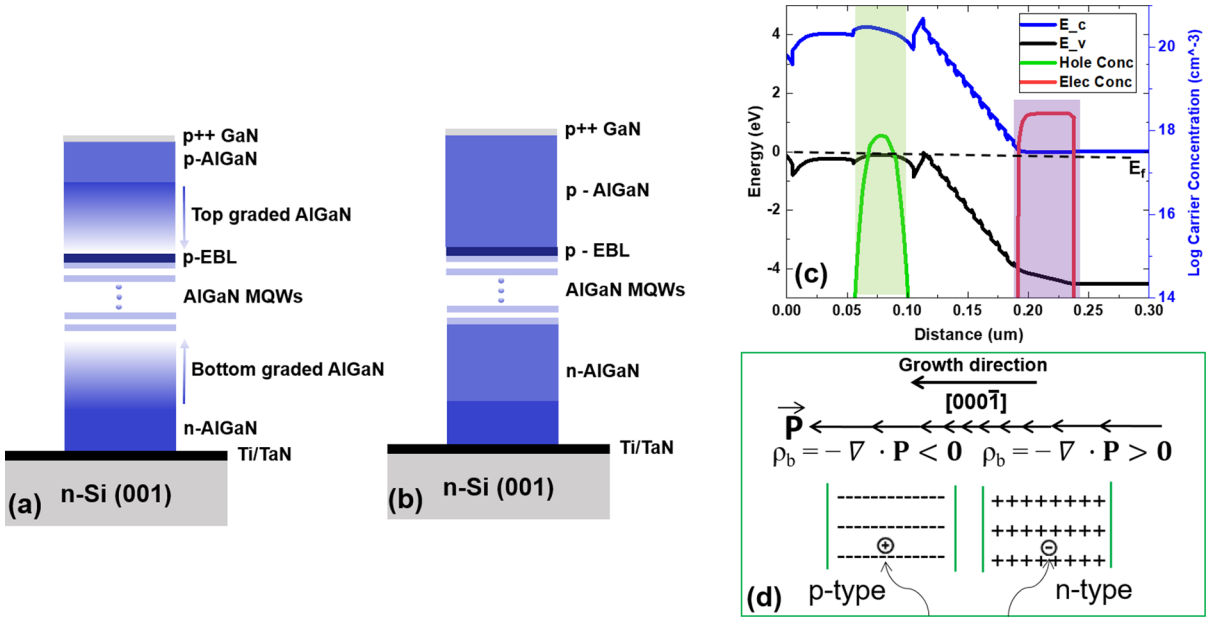

Figure 1. Schematic structures of the (a) GRINSCH diode and (b) conventional p-i-n diode. (c) Simulated energy band diagram of the GRINSCH diode structure with 10 MQWs under thermal equilibrium and electron and hole concentrations in compositionally graded AlGaN layers. (d) Schematic illustration of polarization-induced n-type (positive polarization charge at bottom grading AlGaN layer) and polarization-induced p-type (negative charge at top grading AlGaN layer) in the GRINSCH diode along the [000$\bar{1}$] crystallographic direction (N-polarity). It also shows that a continuous change in the polarization vector in the growth direction creates polarization charge fields.

suggesting an approximately 20−25% of the Al-content in the QW and the $Al_yGa_{1-y}N$ quantum barriers (Al and Ga BEPs of 2×10^{-8} and 3×10^{-8} Torr, hence, $y > x$) with thicknesses of ∼3 and ∼6 nm, respectively, grown at 630 °C. After the growth of a p-AlGaN electron blocking layer (EBL) at 600 °C, p-AlGaN layers were then grown at 610 °C with Al and Ga BEPs of 2×10^{-8} and 3×10^{-8} Torr, respectively, while the Mg cell temperature was kept at 360 °C with the same nitrogen plasma condition. An additional highly doped p-GaN contact layer was grown by increasing the Mg cell temperature to 380 °C and reducing the growth temperature to 580 °C. All layers were grown under N-rich conditions. The $Al_zGa_{1-z}N$ graded layers were grown by linearly changing the temperature of the Ga effusion cell on the basis of the beam-flux calibration. The Ga flux increased linearly from 2×10^{-8} to 4.5×10^{-8} Torr for the bottom grading layer and decreased from 4.5×10^{-8} to 2×10^{-8} Torr for the top grading layer. At the same time, the Al flux was maintained at 2×10^{-8} Torr. For the comparison of GRINSCH and conventional diodes, the same procedure and growth conditions were applied including the same heater and cell temperatures at each stage of the growth.

The devices were fabricated using standard UV contact-lithography techniques.[47] Immediately after the lithography, the sample was dipped in 20% HF to remove surface oxidation before Ni/Au (5 nm/5 nm) blanket-evaporation and annealed in 1 min at 600 °C using rapid thermal processing after evaporation. Further evaporation of Ni/Au (10 nm/200 nm) was carried out to define contact-fingers and probe-pads using photoresist and UV contact lithography. Finally, the Si back-surface was etched away by 200 nm using inductively coupled plasma reactive-ion etching (ICP RIE) in preparation for depositing Ti/Au (10 nm/150 nm) n-contacts. Temperature-dependent photoluminescence (PL) measurements were performed, and the samples were excited with a third harmonic mode (∼260 nm) of mode-locked Ti:sapphire oscillator operating at ∼780 nm. The PL signal was collected by using a UV objective and then measured by an OceanOptics QEPro spectrometer. Electroluminescent (EL) signal was also measured, and the current was injected by using a Keithley source 2450C operating in continuous mode at different injection currents. Scanning electron microscopy (SEM) and scanning transmission electron microscopy (STEM) were used to investigate the quality and structure of the nanowires. SEM images were taken using Zeiss Supra 40. A Thermofisher USA (former FEI) Titan Themis Z microscope was utilized for STEM characterization. The microscope was operated at the accelerating voltage of 300 kV. Atomic-number sensitive (Z-contrast) STEM was realized by acquiring the data with high-angle annular dark-field (HAADF) detector. The equilibrium energy band diagram and the carrier distribution profiles (both electrons and holes) across the entire structure were simulated and analyzed using the commercially available software package Crosslight APSYS program.[48−50] The energy band diagram of the structure was obtained by self-consistently solving Poisson's equation under thermal equilibrium condition, meanwhile taking into account of the existence of strong spontaneous and piezoelectric polarization charges in the AlGaN alloys. For valence band, the 6×6 $k \cdot p$ method was adopted, taking into account the nonparabolic nature of the energy bands. The optical mode profile and optical confinement were computed by numerical solution finite-difference-time-domain (FDTD) software package.

RESULTS AND DISCUSSION

Structural Design and Characterization. Here, we have demonstrated two different types of AlGaN nanowire diode structures: compositionally graded AlGaN layers embedded in nanowires (denoted as GRINSCH diode) and conventional p-i-n nanowires. The sequence of layers in both diodes is schematically illustrated in Figure 1a and b, respectively. The GRINSCH diode consists of a 250 nm n-$Al_{0.5}Ga_{0.5}N$ layer, a 50

DOI: 10.1021/acsphotonics.8b00538
ACS Photonics 2018, 5, 3305−3314

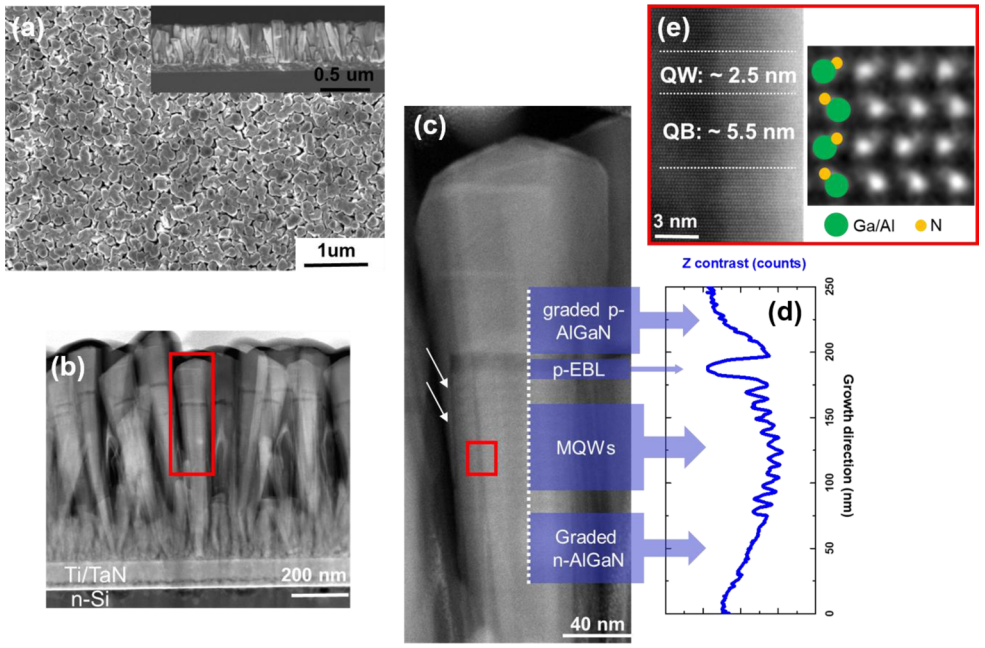

Figure 2. (a) Top-view and cross-sectional (inset) SEM images of GRINSCH diode. (b) Cross-sectional HADDF-STEM image of GRINSCH diode. (c) Enlarged STEM image marked in red rectangular in (b), showing a single nanowire. The white arrows mark the shell of the nanowire. (d) *Z*-contrast profile of the dashed line marked in (c), the darker area indicates higher Al content. (e) Atomic resolution STEM image of the quantum well and barrier (red square marked in (c)) with the atomic arrangement of Al/Ga and nitrogen atoms along the growth direction schematically.

nm Si-doped graded $Al_zGa_{1-z}N$ layer with decreasing the Al composition from 50% to 30% toward the growth direction, followed by 10 pairs $Al_xGa_{1-x}N/Al_yGa_{1-y}N$ multiple quantum wells (MQWs). This is followed by a ∼8 nm high Al-content Mg-doped AlGaN electron blocking layer (EBL) and a 50 nm Mg-doped reversed graded $Al_xGa_{1-x}N$ layer with increasing Al content from 30% to 50%. Finally, a 40 nm Mg-doped $Al_{0.4}Ga_{0.6}N$ layer and a very thin (∼3 nm) heavily doped p-GaN contact layer were grown. The design of the conventional p-i-n diode is similar to the GRINSCH diode, but the bottom- and top-graded AlGaN layers were replaced by an AlGaN layer with 40% of Al content.

The energy band diagram (under thermal equilibrium) and the profile of the polarization-induced electron and hole distribution in the GRINSCH diode are included in Figure 1c. Typically, the MBE-grown nitride nanowires possess N-polarity due to the N-rich condition. Thus, a compositional gradient of decreasing Al-content from 50% to 30% along the growth direction $[000\bar{1}]$ creates a positive polarization charge field as the magnitude of the polarization field varies slowly, resulting in a fixed 3D space bound charge $\rho_b = -\nabla\cdot\mathbf{P}$ (nonzero gradient of the polarization vector $\mathbf{P}$).[26] These positive space charges attract free electrons from surrounding materials (e.g., surface states, defects, dopants), and consequently, a 3D electron gas reservoir is formed, realizing an n-type conductivity of the graded AlGaN layer (as shown in Figure 1d, right). Similarly, in the symmetric part (p-AlGaN layer) of the graded structure where the Al-content is increased linearly from 30% to 50% after the active region growth, a constant negative polarization charge across the graded region is formed. Then, an equivalent amount of free holes are induced, spreading over the graded AlGaN layer, by the polarization field to neutralize these negative charges, giving rise to a mobile 3D hole gas (Figure 1d, left) and, thus, p-type doping is realized.[27,28] Such polarization-induced doping technique is feasible to directly control the density of free electron/hole charges by varying either the Al-content and the AlGaN thickness.[27] Furthermore, a p−n junction can be realized by simply grading AlGaN layers without using conventional impurity doping.[22,28] Moreover, the realization of polarization doping does not freeze out at low temperature due to field ionization, so the electron and hole concentration can be enhanced, independent of temperature.[26] These advantages of polarization doping offer a unique solution to effectively increase both the carrier concentration and the mobility by reducing ionized impurity scattering.[26,28] Most importantly, the inclusion of additional impurities (donors or acceptors) along with polarization doping could further enhance the electrical conductivity of n- and p-type AlGaN layers.[23,24,51]

The calculated band diagram indicates the formation of a p−n junction due to polarization-induced p- and n-type doping of the AlGaN graded layers on either side of the active region.[22,23] Shown in the same figure (Figure 1c) are also the concentration of holes and electrons induced by polarization doping. It should be stressed that such a high concentration of electrons and holes ($1-2 \times 10^{18}$ cm^{-3}) in the p−n junction is obtained without the utilization of intentional impurities and dopants. This doping level in both sides of the junction assumes the existence of a sufficient amount of acceptor-like or donor-like impurities or defects (including surface charges) in either side of the junction, which can be ionized by polarization.[16,24,26,28] In reality, such impurities or defects may occur naturally during the growth process or may be introduced intentionally by incorporating n-type dopants (Si) in the first AlGaN compositionally graded layer and p-type dopants (Be or Mg) in the second AlGaN compositionally graded layer.[26] The effectiveness of this polarization doping (or polarization-enhanced doping) technique has been previously demonstrated in planar UVLEDs.[23,26,28]

DOI: 10.1021/acsphotonics.8b00538
ACS Photonics 2018, 5, 3305−3314

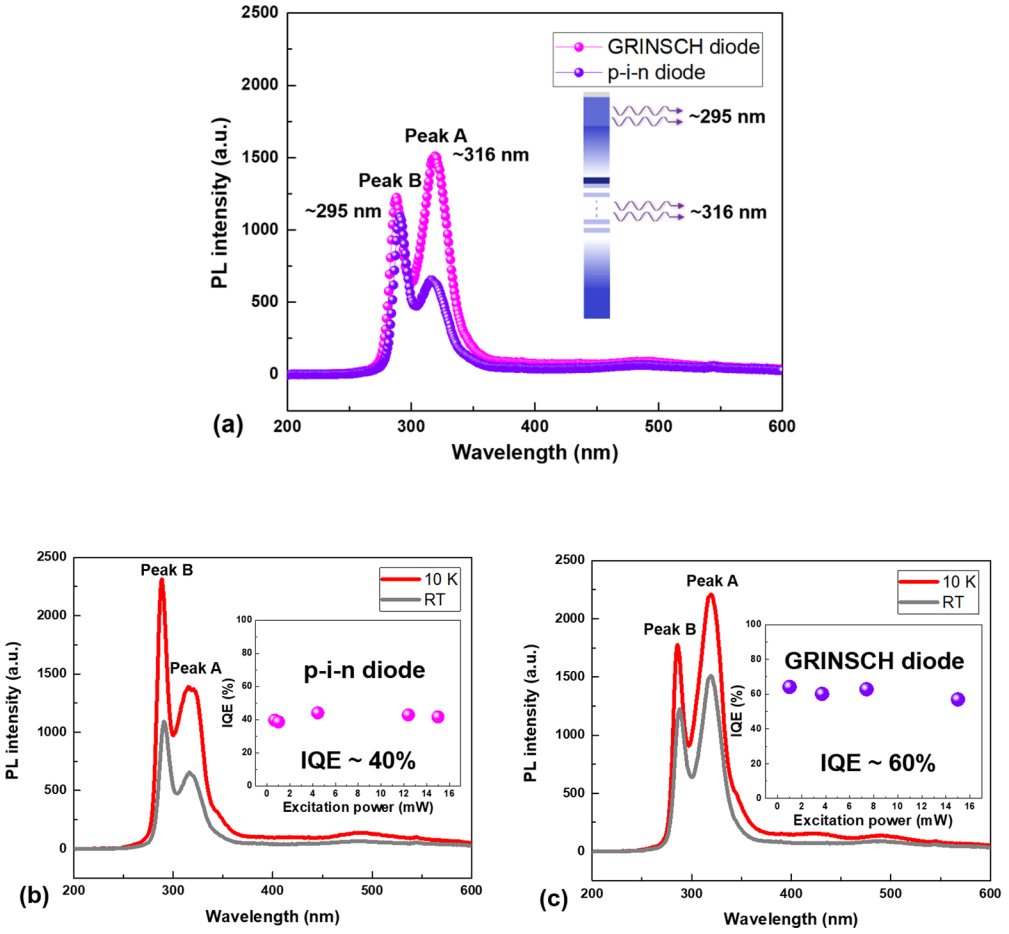

Figure 3. (a) PL spectra of the GRINSCH diode and p-i-n diode at room temperature (RT). PL spectra measured under an excitation power of ~4 mW at RT and 10 K for (b) GRINSCH and (c) p-i-n diode. The inset shows the internal quantum efficiency vs excitation power.

Illustrated in Figure 2a is the SEM image of the GRINSCH nanowires. The nanowires are vertically aligned on the Ti/TaN-coated Si substrate and exhibit relatively uniform height and size distribution (the lateral size is in the range of 120–150 nm and a height of ~750 nm) which is further confirmed by the cross-sectional STEM image (Figure 2b). No interface delamination is observed between the Ti/TaN metal-bilayer and Si substrate, resulting in a relatively uniform nanowire distribution across the entire wafer. The filling factor is estimated to be 96%, representing extremely compact and high-density nanowires. The nearly coalesced nanowires at the top surface provide a simplified fabrication process that we can deposit metal pads directly without using any filling materials to planarize the nanowires.[45] It has to be stressed that a surface planarization step by filling the gaps between nanowires using a polymer (e.g., parylene or polyimide) before depositing metal pads is commonly implemented in fabricating nanowire-based devices.[45,46] However, this planarization process may oxidize the top p-GaN layer during the etch-back procedure which may cause serious damage to the device during the operation. Figure 2c shows an enlarged image of the GRINSCH nanowire with the clear observation the formation Al-rich shell (pointed by the white arrows). Such a spontaneously formed large bandgap AlGaN shell on the sidewall of each nanowire suppress the nonradiative surface recombination and could act as a self-passivated layer to reduce surface states for the visible/UV LEDs and lasers.[52,53] The *Z*-contrast profile shows the integrity of GRINSCH diode nanowire including both graded AlGaN layers, MQWs, and the other part of the structure. Due to the low Al-content difference (only 10%), the color contrast between the QW and barrier layer is hardly noticeable. The nanowires in the conventional p-i-n diode exhibit similar structural properties. Nanowires in both diodes were grown along the *c*-axis and possess N-polarity which is commonly observed in the MBE-grown nanowires, as confirmed in the atomic resolution image of the quantum well and barrier in Figure 2e.

Photoluminescence and Electroluminescence Characterization. Temperature-dependent PL measurements of the investigated GRINSCH and p-i-n diode were performed. Shown in Figure 3a, the nanowires heterostructure exhibits strong emission at ~316 nm (Peak A) with fwhm values of 19.8 and 19.1 nm for the GRINSCH and p-i-n diode, respectively. A slight broadening of the PL spectrum of the GRINSCH diode could be attributed to the graded AlGaN layer where it may have compositional inhomogeneities along the grading direction. These values of the fwhm are similar to the reported AlGaN-based nanowire UV emitters,[17,41,44,52] suggesting the good quality of the nanowires. Emission from the higher Al-content AlGaN nanowire segment (mainly from the top p-AlGaN layer) can also be observed (Peak B: ~ 295 nm). The ratio of Peaks A and B is 1.24 and 0.58 for the GRINSCH- and p-i-n-diode, respectively. The high-luminescence intensity of the GRINSCH diode from the active region could be directly related to the significantly improved carrier flow into quantum wells assisted by the graded AlGaN layers

DOI: 10.1021/acsphotonics.8b00538
ACS Photonics 2018, 5, 3305–3314

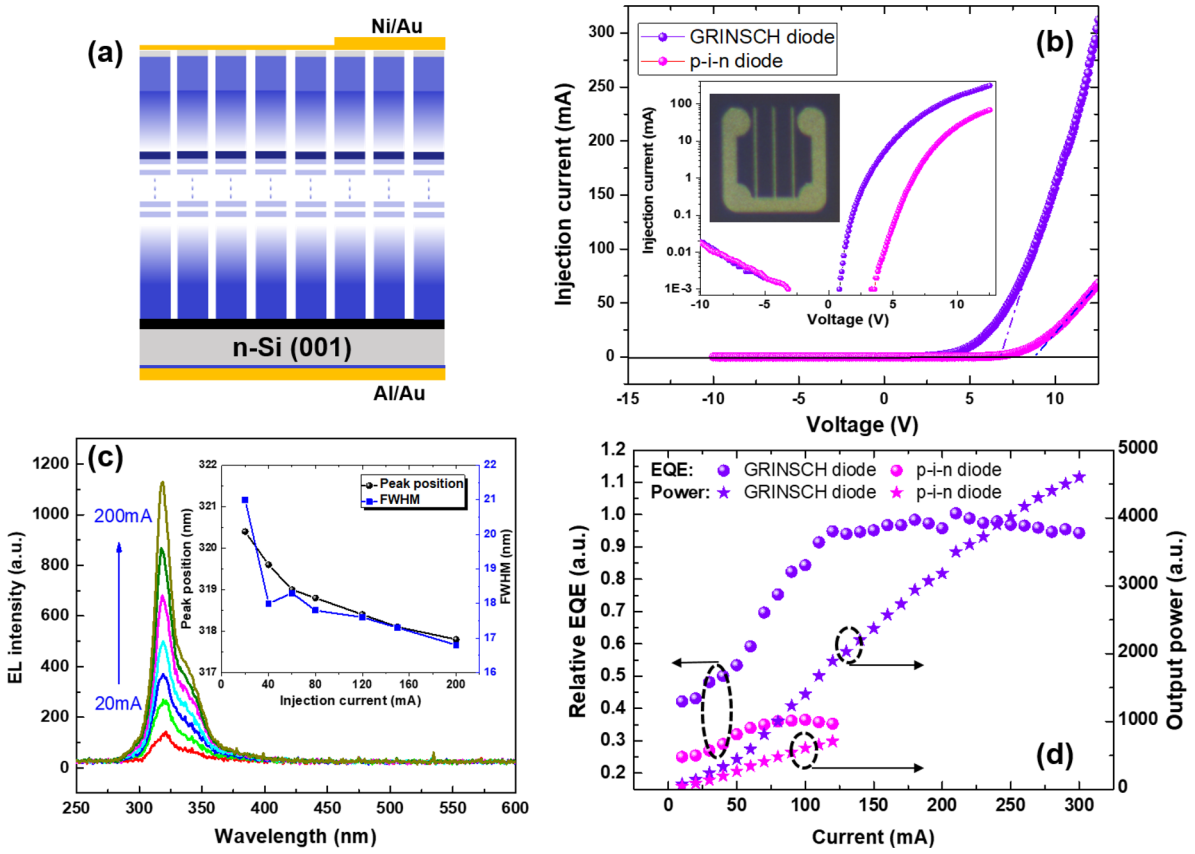

Figure 4. (a) 2D schematic illustration of the fabricated AlGaN nanowire diode on Ti/TaN-coated Si substrate. (b) Current−voltage characteristic of the GRINSCH and p-i-n diode. The inset shows the semilog plots of the $I-V$ curves and an optical image of a GRINSCH diode. (c) EL spectra of the GRINSCH diode varying injection current from 20 to 200 mA. The inset shows the fwhm and peak position of the EL spectra under the same range of injection current. (d) Measured output power and relative EQE of the GRINSCH and p-i-n diodes under the biasing current from 10 to 300 mA. Due to the high resistivity of AlGaN nanowires in the p-i-n diode, the maximum injection current can only reach 120 mA.

and thus higher recombination in the active region. Furthermore, the internal quantum efficiency (IQE) is also estimated by dividing the integrated PL intensity at RT with that measured at 10 K, as shown in Figure 3b,c. The IQE of the GRINSCH diode is nearly 50% higher than the p-i-n diode over a large range of excitation power. Earlier studies in traditional compound semiconductors, such as GaAs and InP-based GRINSCH laser diodes show much lower optical and electrical pumping thresholds compared with abrupt heterojunctions.[54,55] This is mainly attributed to the additional photogenerated carriers in the grading layer.[56,57] These carriers flow into the active region, creating higher luminance performance similar to the observation of a higher intensity of Peak B in the AlGaN GRINSCH diode.

The light−current−voltage ($L-I-V$) characteristics of both GRINSCH and p-i-n diodes are measured under different injection current under continuous-wave (CW) biasing conditions. Figure 4a depicts the fabricated device. Because of the nearly coalesced (filling factor ∼ 96%) top surface of the nanowires (as shown in the Figure 2a), we simply employed a standard photolithography procedure to define the current spreading layer for the hole injection.[47] The Al/Au and Ni/Au metal stack was deposited directly to the n-Si substrate and p-GaN layer to form an ohmic contact, respectively. The device mesa size is 500 × 500 μm^2 for both diodes. From the $I-V$ characteristics, it can be seen that both diodes show a usual rectifying behavior. Noted in Figure 4b, the turn-on voltage is around 6.5 V for the GRINSCH diode, whereas it is 8.9 V for the p-i-n diode. A similar leakage current is observed in both diodes, as shown in the inset of Figure 4b. Most importantly, the series resistance, which is extracted from the slope of the $I-V$ characteristic in the linear region between 10 and 12.5 V for both diodes, is as low as 16.7 Ω in the GRINSCH diode, nearly four time smaller than the one in the p-i-n diode (∼58.1 Ω). This significant reduction of the series resistance is attributed to the pronounced resistivity reduction of the body of the AlGaN nanowires owing to the effective polarization-induced n- and p-doping by incorporating the compositionally graded AlGaN layers adjacent to the active region. In the GRINSCH configuration, in addition to the thermally activated electrons and holes from the Si-donors and Mg-acceptors, polarization-induced doping also provides ionizing donor and acceptor dopants using the intrinsic built-in electronic polarization in the AlGaN crystals, as confirmed by its band diagram (Figure 1c).[26] Because of the major improvement in the n- and p-type electrical conductivity, a lower turn-on voltage and smaller sheet resistance are expected, which is similar to the previous reports in the planar UVLED structures.[23,26]

Shown in Figure 4c is the EL spectra measured under various injection currents under CW biasing condition for GRINSCH diode. A relatively narrow emission peak centered at 318 nm was measured. The spectral line width (full width at half-maximum: fwhm) is ∼20 nm at the 20 mA and reduced to ∼17 nm when the current is increased up to 200 mA. This relatively small value of fwhm is close to the one reported in

DOI: 10.1021/acsphotonics.8b00538
ACS Photonics 2018, 5, 3305−3314

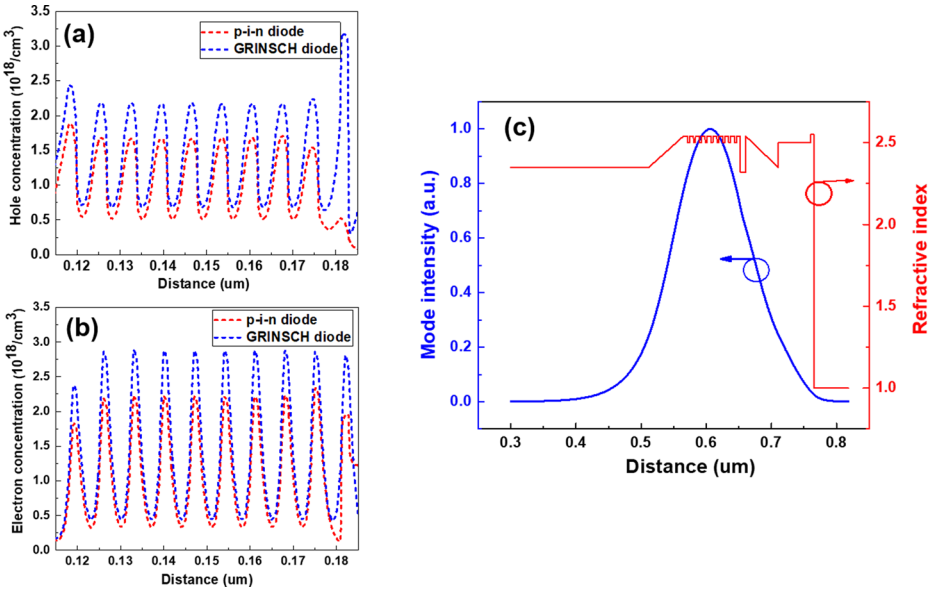

Figure 5. (a) Hole and (b) electron concentrations for the GRINSCH diode (blue dash line) and the conventional diode (red dash line) at 200 mA; (c) Vertical profile of the index of refraction and the optical mode profile for the GRINSCH diode.

UVLEDs incorporating planar AlGaN MQWs in similar peak emission regime.[18,58,59] A blue shift of ∼3 nm in the emission wavelength was measured with increasing injection current, indicating small quantum-confined Stark effect. No defect-related emission in the visible spectral range was observed. The output power of nanowire diodes was measured directly on the wafer without any packaging under CW biasing. Shown in Figure 4d, the output power continuously rises as the injection current increases for the GRINSCH diode. Noticeably, the GRINSCH diodes sustain the injection current as high as 320 mA compared to the conventional p-i-n diode (120 mA) for the device size 500 × 500 um^2. Such drastically improved electrical injection and output power of the GRINSCH diode is attributed to the significantly enhanced electron/hole transport and injection into the active region because of the polarization induced doping. The relative external quantum efficiency (EQE), is measured by taking the ratio of the number of emitted photons over the number of injected electrons. EQEs of both diodes versus injection current under CW operation are presented in Figure 4d. For the conventional p-i-n diode, the device operation saturated immediately at low current injection due to its low conductivity of the nanowires themselves, resulting in low output power and low EQE performance. Nevertheless, in GRINSCH diode, EQE increases almost linearly with the increase in injection current up to 120 mA. It then plateaus up to 320 mA. We did not observe any significant efficiency droop as observed in the conventional p-i-n diode. Normally, the severe efficiency droop has been commonly measured in planar AlGaN-based LED devices.[58,59] The underlying mechanism for this droop may include Auger recombination and electron overflow at high injection current.[3] Such droop was also observed in our previous study where the AlGaN nanowires were grown directly on Si substrates.[47] It is reasonable to claim that NWs grown on Ti/TaN-coated Si substrate have better thermal conductivity, which helps to dissipate heat efficiently at high injection current compared to the ones grown on conventional Si or sapphire substrates. Therefore, the nanowires grown on metal substrates or on metal-coated substrates are desirable for high-current injection light-emitting devices. It is expected that with further optimization of the design and epitaxy process of AlGaN nanowires, both the turn-on voltage and resistance of nanowire diodes in the GRINSCH configuration can be further reduced.

Step Toward UV Laser Diode Implementation. Previously, such a GRINSCH diode configuration has been implemented in conventional III−V compounds-based (e.g., GaAs, InP) devices, particularly in laser diodes, by virtue of the simultaneous improvement of carrier injection and vertical optical mode confinement, as pioneered by the Kazarinov et al. and Tsang et al.[54,55] GaAs and InP-based GRINSCH laser diodes, with either linear or parabolic shape of the graded-index profile, have achieved extremely low threshold currents and thus have been commercialized in semiconductor industry.[56,57] Recently, a GRINSCH-based InGaN laser diode was also demonstrated, showing very promising low threshold current density of 3.5 kA/cm^2, compared with the classical step-index structure.[60] However, for the aforementioned devices, the advantage of polarization doping technique has not been taken into account because both n- and p-doing are easily achieved in the InGaN layers. For the realization of electrically pumped AlGaN-based laser diode, we face a tremendous challenge to obtain a conductive p-type Al-rich AlGaN layer because of the high ionization energies of Mg-acceptors. Thus, any breakthrough in the development of electrically injected UV semiconductor laser diode will highly depend on the capability to efficiently p-dope high Al content AlGaN layers. Therefore, a semiconductor UV laser diode design, which can take advantage of the polarization-enhanced p-type doping via compositional gradient of Al-content in the AlGaN layers while achieving better carrier and optical mode confinement is a structure having the GRINSCH configuration.[61,62]

Figure 5a,b show the calculated hole and electron concentrations under a current injection of 200 mA for both diode, respectively. Significant increases in the hole and electron concentrations by 81.1% and 29.5%, respectively, can be expected in the GRINSCH diode compared with the

DOI: 10.1021/acsphotonics.8b00538
ACS Photonics 2018, 5, 3305−3314

traditional p-i-n one. Such improvement is attributed to better carrier confinement and possibly high current injection efficiency with the aid of the polarization-induced doping due to compositionally graded AlGaN layers on either side of the active region. Furthermore, the near-field optical model profile and the vertical profile of the index refraction in the GRINSCH diode are depicted in Figure 5c, computed by the FDTD numerical simulation. Refractive indices were extracted from Brunner et al.[63] for the AlGaN and graded $Al_xGa_{1-x}N$ layers at the targeted emission wavelength of 315 nm. The optical mode is well confined by the graded AlGaN layers, with an optical confinement factor, Γ, in the active region of the device of 17.9%. Such a large optical confinement value could provide the confidence of the suitable laser structure by adopting GRINSCH configuration, as most of the reported AlGaN MQW-based lasers has only 1−3% optical confinement.[8,9] Admittedly, further optimization of the active region, such as the number of QWs as well as the thickness of each QW and QB layer, is also critical to achieve single mode lasing with the reduced internal material loss.[62]

The above results show a feasible approach to realize UV laser diode using the AlGaN-based GRINSCH configuration, especially the demonstration of efficient high current injection and reduced series resistance, we still face challenges in fabricating such nanowire-based laser diodes. On the basis of the extreme surface sensitivity due to large surface to volume of nanowires and the fact that difficulty in fabricating high reflectivity mirrors for lasing, extensive efforts are required to overcome these obstacles. Recently, InGaN nanowire structures, including green and red edge emitting lasers have been reported,[64,65] thus, the present effort paves the way toward the realization of UV laser diode based on dislocation-free nanowires.

CONCLUSION

In this context, a novel AlGaN-nanowires-based diode by adopting GRINSCH configuration in which we embedded the active region between two compositionally graded AlGaN layers was proposed and characterized. We demonstrated that the AlGaN-based GRINSCH diode, with the nearly coalesced surface (filling factor > 96%), possesses encouraging electrical and optical performance compared to the conventional p-i-n diode. A lower turn-on voltage of 6.5 V and significant reduction of the series resistance by almost four times in the GRINSCH diode are achieved. Such improved electrical characteristics show strong evidence of the effectiveness of polarization-induced n- and p-doping in the compositionally graded AlGaN layers which eventually enhance the carrier injection efficiency. The numerical analysis indicates a higher electron and hole concentrations in the active region and large optical confinement for the GRINSCH diode. Therefore, the proposed GRINSCH diode brings us one step forward to the eventual demonstration of AlGaN-based laser diodes.

AUTHOR INFORMATION

Corresponding Authors

*E-mail: haiding.sun@kaust.edu.sa.
*E-mail: boon.ooi@kaust.edu.sa.
*E-mail: xiaohang.li@kaust.edu.sa.

ORCID

Haiding Sun: 0000-0001-8664-666X
Chao Zhao: 0000-0002-9582-1068
Jae-Hyun Ryou: 0000-0002-7397-6616
Xixiang Zhang: 0000-0002-3478-6414
Xiaohang Li: 0000-0002-4434-365X

Notes

The authors declare no competing financial interest.

ACKNOWLEDGMENTS

We acknowledge the financial support from King Abdullah University of Science and Technology (KAUST) baseline funding, BAS/1/1614-01-01, BAS/1/1664-01-01, BAS/1/1376-01-01, and KAUST CRG URF/1/3437-01-01. Also, B.S.O., T.K.N., R.C.S., M.K.S., C.Z., J.W.M., and D.P. gratefully acknowledge funding support from King Abdulaziz City for Science and Technology, Grant No. KACST TIC R2-FP-008 and KAUST MBE equipment funding, C/M-20000-12-001-77. The work at University of Houston was supported by King Abdullah University of Science and Technology (KAUST; Contract No.: OSR-2017-CRG6-3437.02). J.H.R. also acknowledges partial financial support from the Texas Center for Superconductivity at the University of Houston (TcSUH). H.S. greatly appreicates the help and fruitful discussion from Prof. Theodore D. Moustakas at Boston University (Boston, MA, United States) in carrying out the project.

REFERENCES

(1) Khan, A.; Balakrishnan, K.; Katona, T. Ultraviolet light-emitting diodes based on group three nitrides. *Nat. Photonics* **2008**, *2*, 77−84.
(2) Li, X.; Xie, H.; Ryou, J. H.; Ponce, F. A.; Detchprohm, T.; Dupuis, R. D. Onset of surface stimulated emission at 260 nm from AlGaN multiple quantum wells. *Appl. Phys. Lett.* **2015**, *107*, 241109.
(3) Kneissl, M.; Rass, J. *III-Nitride Ultraviolet Emitters*; Springer: Switzerland, 2016; Chapter 1, pp 1−25.
(4) Kamiyama, S.; Iwaya, M.; Hayashi, N.; Takeuchi, T.; Amano, H.; Akasaki, I.; Watanabe, S.; Kaneko, Y.; Yamada, N. Low-temperature-deposited AlGaN interlayer for improvement of AlGaN/GaN heterostructure. *J. Cryst. Growth* **2001**, *223*, 83−91.
(5) Park, J. H.; Kim, D. Y.; Schubert, E. F.; Cho, J.; Kim, J. K. Fundamental limitations of wide-bandgap semiconductors for light-emitting diodes. *ACS Energy Lett.* **2018**, *3*, 655−662.
(6) Taniyasu, Y.; Kasu, M.; Makimoto, T. An aluminium nitride light-emitting diode with a wavelength of 210 nanometres. *Nature* **2006**, *441*, 325−328.
(7) Nakarmi, M. L.; Nepal, N.; Lin, J. Y.; Jiang, H. X. Photoluminescence studies of impurity transitions in Mg-doped AlGaN alloys. *Appl. Phys. Lett.* **2009**, *94*, 091903.
(8) Yoshida, H.; Yamashita, Y.; Kuwabara, M.; Kan, H. A 342-nm ultraviolet AlGaN multiple-quantum-well laser diode. *Nat. Photonics* **2008**, *2*, 551.
(9) Yoshida, H.; Yamashita, Y.; Kuwabara, M.; Kan, H. Demonstration of an ultraviolet 336 nm AlGaN multiple-quantum-well laser diode. *Appl. Phys. Lett.* **2008**, *93*, 241106.
(10) Ebata, K.; Nishinaka, J.; Taniyasu, Y.; Kumakura, K. High hole concentration in Mg-doped AlN/AlGaN superlattices with high Al content Jpn. *J. Appl. Phys.* **2018**, *57*, 04FH09.
(11) Cheng, B.; Choi, S.; Northrup, J. E.; Yang, Z.; Knollenberg, C.; Teepe, M.; Wunderer, T.; Chua, C. L.; Johnson, N. M. Enhanced vertical and lateral hole transport in high aluminum-containing AlGaN for deep ultraviolet light emitters. *Appl. Phys. Lett.* **2013**, *102*, 231106.
(12) Martens, M.; Kuhn, C.; Ziffer, E.; Simoneit, T.; Kueller, V.; Knauer, A.; Rass, J.; Wernicke, T.; Einfeldt, S.; Weyers, M.; Kneissl, M. Low absorption loss p-AlGaN superlattice cladding layer for current-injection deep ultraviolet laser diodes. *Appl. Phys. Lett.* **2016**, *108*, 151108.

DOI: 10.1021/acsphotonics.8b00538
ACS Photonics 2018, 5, 3305−3314

(13) Tahtamouni, T. M. A.; Lin, J. Y.; Jiang, H. X. Effects of Mg-doped AlN/AlGaN superlattices on properties of p-GaN contact layer and performance of deep ultraviolet light emitting diodes. *AIP Adv.* **2014**, *4*, 047122.
(14) Wang, X.; Wang, W.; Wang, J.; Wu, H.; Liu, C. Experimental evidences for reducing Mg activation energy in high Al-content AlGaN alloy by MgGa δ doping in $(AlN)_m/(GaN)_n$ superlattice. *Sci. Rep.* **2017**, *7*, 44223.
(15) Chen, Y.; Wu, H.; Han, E.; Yue, G.; Chen, Z.; Wu, Z.; Wang, G.; Jiang, H. High hole concentration in p-type AlGaN by indium-surfactant-assisted Mg-delta doping. *Appl. Phys. Lett.* **2015**, *106*, 162102.
(16) Liang, Y. H.; Towe, E. Heavy Mg-doping of (Al,Ga)N films for potential applications in deep ultraviolet light-emitting structures. *J. Appl. Phys.* **2018**, *123*, 095303.
(17) Sadaf, S. M.; Zhao, S.; Wu, Y.; Ra, Y.-H.; Liu, X.; Vanka, S.; Mi, Z. An AlGaN core-shell tunnel junction nanowire light-emitting diode operating in the ultraviolet-C band. *Nano Lett.* **2017**, *17*, 1212−1218.
(18) Zhang, Y.; Krishnamoorthy, S.; Johnson, J. M.; Akyol, F.; Allerman, A.; Moseley, M. W.; Armstrong, A.; Hwang, J.; Rajan, S. Interband tunneling for hole injection in III-nitride ultraviolet emitters. *Appl. Phys. Lett.* **2015**, *106*, 141103.
(19) Wood, C.; Jena, D. *Polarization Effects in Semiconductors: From Ab Initio Theory to Device; Applications*; Springer Science & Business Media, 2007; Chapter 4, pp 161−216.
(20) Fang, Y.; Feng, Z.; Yin, J.; Zhou, X.; Wang, Y.; Gu, G.; Song, X.; Lv, Y.; Li, C.; Cai, S. AlGaN/GaN Polarization-doped field-effect transistors with graded heterostructure IEEE Trans. *IEEE Trans. Electron Devices* **2014**, *61*, 4084−4089.
(21) Wang, W.; Shervin, S.; Oh, S. K.; Chen, J.; Huai, Y.; Pouladi, S.; Kim, H.; Lee, S.-N.; Ryou, J.-H. Flexible AlGaInN/GaN hetero-structures for high-hole-mobility transistors IEEE. *IEEE Electron Device Lett.* **2017**, *38*, 1086−1089.
(22) Sun, H.; Pecora, E. F.; Woodward, J.; Smith, D. J.; Dal Negro, L.; Moustakas, T. D. Effect of indium in $Al_{0.65}Ga_{0.35}N/Al_{0.8}Ga_{0.2}N$ MQWs for the development of deep-UV laser structures in the form of graded index separate confinement heterostructure (GRINSCH). *Phys. Status Solidi A* **2016**, *213*, 1165−1169.
(23) Sun, H.; Moustakas, T. D. UV emitters based on an AlGaN p−n junction in the form of graded-index separate confinement heterostructure. *Appl. Phys. Express* **2014**, *7*, 12104.
(24) Li, S.; Zhang, T.; Wu, J.; Yang, Y.; Wang, Z.; Wu, Z.; Chen, Z.; Jiang, Y. Polarization induced hole doping in graded $Al_xGa_{1-x}N$ (x= 0.7 ∼ 1) layer grown by molecular beam epitaxy. *Appl. Phys. Lett.* **2013**, *102*, 062108.
(25) Armstrong, A. M.; Allerman, A. A. Polarization-induced electrical conductivity in ultra-wide band gap AlGaN alloys. *Appl. Phys. Lett.* **2016**, *109*, 222101.
(26) Simon, J.; Protasenko, V.; Lian, C.; Xing, H.; Jena, D. Polarization-induced hole doping in wide-band-gap uniaxial semi-conductor heterostructures. *Science* **2010**, *327*, 60−64.
(27) Lytvyn, P. M.; Kuchuk, A. V.; Mazur, Y. I.; Li, C.; Ware, M. E.; Wang, Z. M.; Kladko, V. P.; Belyaev, A. E.; Salamo, G. J. Polarization effects in graded AlGaN nanolayers revealed by current-sensing and Kelvin probe microscopy. *ACS Appl. Mater. Interfaces* **2018**, *10*, 6755−6763.
(28) Li, S.; Ware, M.; Wu, J.; Minor, P.; Wang, Z.; Wu, Z.; Jiang, Y.; Salamo, G. J. Polarization induced pn-junction without dopant in graded AlGaN coherently strained on GaN. *Appl. Phys. Lett.* **2012**, *101*, 122103.
(29) Tran, N.; Le, B.; Zhao, S.; Mi, Z. On the mechanism of highly efficient p-type conduction of Mg-doped ultra-wide-bandgap AlN nanostructures. *Appl. Phys. Lett.* **2017**, *110*, 032102.
(30) Zhao, S.; Woo, S. Y.; Bugnet, M.; Liu, X.; Kang, J.; Botton, G. A.; Mi, Z. Three-dimensional quantum confinement of charge carriers in self-organized AlGaN nanowires: A viable route to electrically injected deep ultraviolet lasers. *Nano Lett.* **2015**, *15*, 7801−7807.
(31) Zhao, S.; Connie, A. T.; Dastjerdi, M. H.; Kong, X. H.; Wang, Q.; Djavid, M.; Sadaf, S.; Liu, X. D.; Shih, I.; Guo, H.; Mi, Z. Aluminum nitride nanowire light emitting diodes: Breaking the fundamental bottleneck of deep ultraviolet light sources. *Sci. Rep.* **2015**, *5*, 8332.
(32) Zhao, S.; Le, B.; Liu, D.; Liu, X. D.; Kibria, M.; Szkopek, T.; Guo, H.; Mi, Z. p-Type InN nanowires. *Nano Lett.* **2013**, *13*, 5509−5513.
(33) Perea, D. E.; Hemesath, E. R.; Schwalbach, E. J.; Lensch-Falk, J. L.; Voorhees, P. W.; Lauhon, L. J. Direct measurement of dopant distribution in an individual vapour−liquid−solid nanowire. *Nat. Nanotechnol.* **2009**, *4*, 315−319.
(34) Ho, J. C.; Yerushalmi, R.; Jacobson, Z. A.; Fan, Z.; Alley, R. L.; Javey, A. Controlled nanoscale doping of semiconductors via molecular monolayers. *Nat. Mater.* **2008**, *7*, 62−67.
(35) Xie, P.; Hu, Y.; Fang, Y.; Huang, J.; Lieber, C. M. Diameter-dependent dopant location in silicon and germanium nanowires. *Proc. Natl. Acad. Sci. U. S. A.* **2009**, *106*, 15254−15258.
(36) Koren, E.; Berkovitch, N.; Rosenwaks, Y. Measurement of active dopant distribution and diffusion in individual silicon nanowires. *Nano Lett.* **2010**, *10*, 1163−1167.
(37) Allen, J. E.; Perea, D. E.; Hemesath, E. R.; Lauhon, L. J. Nonuniform nanowire doping profiles revealed by quantitative scanning photocurrent microscopy. *Adv. Mater.* **2009**, *21*, 3067−3072.
(38) Glas, F. Critical dimensions for the plastic relaxation of strained axial heterostructures in free-standing nanowires. *Phys. Rev. B: Condens. Matter Mater. Phys.* **2006**, *74*, 121302.
(39) Galopin, E.; Largeau, L.; Patriarche, G.; Travers, L.; Glas, F.; Harmand, J. C. Morphology of self-catalyzed GaN nanowires and chronology of their formation by molecular beam epitaxy. *Nanotechnology* **2011**, *22*, 245606.
(40) May, B. J.; Selcu, C. M.; Sarwar, A. T. M. G.; Myers, R. C. Nanoscale current uniformity and injection efficiency of nanowire light emitting diodes. *Appl. Phys. Lett.* **2018**, *112*, 093107.
(41) Kent, T. F.; Carnevale, S. D.; Sarwar, A. T.; Phillips, P. J.; Klie, R. F.; Myers, R. C. Deep ultraviolet emitting polarization induced nanowire light emitting diodes with AlxGa1-xN active regions. *Nanotechnology* **2014**, *25*, 455201.
(42) Basanta, R.; Mahesh, K.; Mohana, K. R.; Thirumaleshwara, N. B.; Krupanidhi, S. B. Binary group III-nitride based heterostructures: band offsets and transport properties. *J. Phys. D: Appl. Phys.* **2015**, *48*, 423001.
(43) Ebaid, M.; Min, J.; Zhao, C.; Ng, T. K.; Idriss, H.; Ooi, B. S. Water Splitting over Epitaxially Grown InGaN Nanowires on-Metallic Titanium/Silicon Template: Reduced Interfacial Transfer Resistance and Improved Stability. *J. Mater. Chem. A* **2018**, *6*, 6922.
(44) Priante, D.; Janjua, B.; Prabaswara, A.; Subedi, R. C.; Elafandy, R. T.; Lopatin, S.; Anjum, D. H.; Zhao, C.; Ng, T. K.; Ooi, B. S. Highly uniform ultraviolet-A quantum-confined AlGaN nanowire LEDs on metal/silicon with a TaN interlayer. *Opt. Mater. Express* **2017**, *7*, 4214−4224.
(45) Janjua, B.; Sun, H.; Zhao, C.; Anjum, D. H.; Priante, D.; Alhamoud, A. A.; Wu, F.; Li, X.; Albadri, A. M.; Alyamani, A. Y.; El-Desouki, M. M.; Ng, T. K.; Ooi, B. S. Droop-free $Al_xGa_{1-x}N/Al_yGa_{1-y}N$ quantum-disks-in-nanowires ultraviolet LED emitting at 337 nm on metal/silicon substrates. *Opt. Express* **2017**, *25*, 1381−1390.
(46) Sun, H.; Shakfa, M. K.; Muhammed, M.; Janjua, B.; Li, K. H.; Lin, R.; Ng, T. K.; Roqan, I. S.; Ooi, B. S.; Li, X. Surface-Passivated AlGaN Nanowires for Enhanced Luminescence of Ultraviolet Light Emitting Diodes. *ACS Photonics* **2018**, *5*, 964−970.
(47) Janjua, B.; Sun, H.; Zhao, C.; Anjum, D. H.; Wu, F.; Alhamoud, A. A.; Li, X.; Albadri, A. M.; Alyamani, A. Y.; El-Desouki, M. M.; Ng, T. K.; Ooi, B. S. Self-planarized quantum-disks-in-nanowires ultra-violet-B emitters utilizing pendeo-epitaxy. *Nanoscale* **2017**, *9*, 7805−7813.
(48) Chang, J.-Y.; Chang, H.-T.; Shih, Y.-H.; Chen, F.-M.; Huang, M.-F.; Kuo, Y.-K. Efficient Carrier Confinement in Deep-Ultraviolet Light-Emitting Diodes With Composition-Graded Configuration IEEE Trans. *IEEE Trans. Electron Devices* **2017**, *64*, 4980−4984.

DOI: 10.1021/acsphotonics.8b00538
ACS Photonics 2018, 5, 3305−3314

(49) Zhang, Z. H.; Huang Chen, S. W.; Zhang, Y.; Li, L.; Wang, S. W.; Tian, K.; Chu, C.; Fang, M.; Kuo, H. C.; Bi, W. Hole transport manipulation to improve the hole injection for deep ultraviolet light-emitting diodes. *ACS Photonics* **2017**, *4*, 1846−1850.
(50) Zhang, Z. H.; Li, L.; Zhang, Y.; Xu, F.; Shi, Q.; Shen, B.; Bi, W. On the electric-field reservoir for III-nitride based deep ultraviolet light-emitting diodes. *Opt. Express* **2017**, *25*, 16550−16559.
(51) Liang, Y. H.; Towe, E. Progress in efficient doping of high aluminum-containing group III-nitrides. *Appl. Phys. Rev.* **2018**, *5*, 011107.
(52) Wang, Q.; Connie, A. T.; Nguyen, H. P. T.; Kibria, M. G.; Zhao, S.; Sharif, S.; Shih, I.; Mi, Z. Highly efficient, spectrally pure 340 nm ultraviolet emission from $Al_xGa_{1-x}N$ nanowire based light emitting diodes. *Nanotechnology* **2013**, *24*, 345201.
(53) Zhao, S.; Connie, A. T.; Dastjerdi, M. H. T.; Kong, X. H.; Wang, Q.; Djavid, M.; Sadaf, S.; Liu, X. D.; Shih, I.; Guo, H.; Mi, Z. Aluminum nitride nanowire light emitting diodes: Breaking the fundamental bottleneck of deep ultraviolet light sources. *Sci. Rep.* **2015**, *5*, 8332.
(54) Kazarino, R. F.; Tsarenkov, G. V. Theory of a variable-gap laser. *Sov. Phys. Semicond.* **1976**, *10*, 178−182.
(55) Tsang, W. T. A graded-index waveguide separate-confinement laser with very low threshold and a narrow Gaussian beam. *Appl. Phys. Lett.* **1981**, *39*, 134−137.
(56) Tsang, W. T. Extremely low threshold (AlGa)As modified multiquantum well heterostructure lasers grown by molecular-beam epitaxy. *Appl. Phys. Lett.* **1981**, *39*, 786.
(57) Kasemset, D.; Hong, C.-S.; Patel, N. B.; Dapkus, P. D. Graded barrier single quantum well lasers - Theory and experiment IEEE. *IEEE J. Quantum Electron.* **1983**, *19*, 1025.
(58) Shatalov, M.; Sun, W.; Lunev, A.; Hu, X.; Dobrinsky, A.; Bilenko, Y.; Yang, J.; Shur, M.; Gaska, R.; Moe, C.; Garrett, G.; Wraback, M. AlGaN Deep-Ultraviolet Light-Emitting Diodes with External Quantum Efficiency above 10%. *Appl. Phys. Express* **2012**, *5*, 082101.
(59) Sun, H.; Woodward, J.; Yin, J.; Moldawer, A.; Pecora, E. F.; Nikiforov, A. Y.; Dal Negro, L.; Paiella, R.; Ludwig, K., Jr; Smith, D. J.; Moustakas, T. D. Development of AlGaN-based graded-index-separate-confinement-heterostructure deep UV emitters by molecular beam epitaxy. *J. Vac. Sci. Technol., B: Nanotechnol. Microelectron.: Mater., Process., Meas., Phenom.* **2013**, *31* (3), 03C117.
(60) Stańczyk, S.; Czyszanowski, T.; Kafar, A.; Goss, J.; Grzanka, S.; Grzanka, E.; Czernecki, R.; Bojarska, A.; Targowski, G.; Leszczyński, M.; Suski, T.; Kucharski, R.; Perlin, P. Graded-index separate confinement heterostructure InGaN laser diodes. *Appl. Phys. Lett.* **2013**, *103*, 261107.
(61) Pecora, E. F.; Sun, H.; Negro, L. D.; Moustakas, T. D. Deep-UV optical gain in AlGaN-based graded-index separate confinement heterostructure. *Opt. Mater. Express* **2015**, *5*, 809.
(62) Sun, H.; Yin, J.; Pecora, E. F.; Negro, L. D.; Paiella, R.; Moustakas, T. D. Deep-Ultraviolet Emitting AlGaN Multiple Quantum Well Graded-Index Separate-Confinement Heterostructures Grown by MBE on SiC Substrates. *IEEE Photonics J.* **2017**, *9*, 2201109.
(63) Brunner, D.; Angerer, H.; Bustarret, E.; Freudenberg, F.; Höpler, R.; Dimitrov, R.; Ambacher, O.; Stutzmann, M. Optical constants of epitaxial AlGaN films and their temperature dependence. *J. Appl. Phys.* **1997**, *82*, 5090−5096.
(64) Frost, T.; Jahangir, S.; Stark, E.; Deshpande, S.; Hazari, A.; Zhao, C.; Ooi, B. S.; Bhattacharya, P. Monolithic electrically injected nanowire array edge-emitting laser on (001) silicon. *Nano Lett.* **2014**, *14*, 4535−4541.
(65) Jahangir, S.; Frost, T.; Hazari, A.; Yan, L.; Stark, E.; LaMountain, T.; Millunchick, J. M.; Ooi, B. S.; Bhattacharya, P. Small signal modulation characteristics of red-emitting (λ= 610 nm) III-nitride nanowire array lasers on (001) silicon. *Appl. Phys. Lett.* **2015**, *106*, 071108.

DOI: 10.1021/acsphotonics.8b00538
ACS Photonics 2018, 5, 3305−3314